

# A study of the correlations between jet quenching observables at RHIC

Jiangyong Jia,<sup>1,2,\*</sup> W. A. Horowitz,<sup>3,†</sup> and Jinfeng Liao<sup>2,‡</sup>

<sup>1</sup>*Department of Chemistry, Stony Brook University, Stony Brook, NY 11794, USA*

<sup>2</sup>*Physics Department, Brookhaven National Laboratory, Upton, NY 11796, USA*

<sup>3</sup>*Department of Physics, University of Cape Town, Private Bag X3, Rondebosch 7701, South Africa*

(Dated: June 30, 2011)

Focusing on four types of correlation plots,  $R_{AA}$  vs.  $v_2$ ,  $R_{AA}$  vs.  $I_{AA}$ ,  $I_{AA}$  vs.  $v_2^{I_{AA}}$  and  $v_2$  vs.  $v_2^{I_{AA}}$ , we demonstrate how the centrality dependence of *correlations* between multiple jet quenching observables provide valuable insight into the energy loss mechanism in a quark-gluon plasma. In particular we find that a qualitative energy loss model gives a good description of  $R_{AA}$  vs.  $v_2$  only when we take  $\Delta E \sim l^3$  and a medium geometry generated by a model of the Color Glass Condensate. This same  $\Delta E \sim l^3$  model also qualitatively describes the trigger  $p_T$  dependence of  $R_{AA}$  vs.  $I_{AA}$  data and makes novel predictions for the centrality dependence for this  $R_{AA}$  vs.  $I_{AA}$  correlation. Current data suggests, albeit with extremely large uncertainty, that  $v_2^{I_{AA}} \gg v_2$ , a correlation that is difficult to reproduce in current energy loss models.

PACS numbers: 12.38.Mh, 24.85.+p, 25.75.-q

Keywords: Relativistic heavy-ion collisions, Quark-gluon plasma, Jet quenching, Jet Tomography

**Introduction:** The combination of theoretical predictions and experimental measurements of high- $p_T$  jet observables provides a unique basis for determining the properties of the strongly-interacting quark gluon plasma (sQGP) created in Au+Au collisions at the Relativistic Heavy Ion Collider (RHIC) [1–3]. After nearly a decade long effort, jet quenching via final state partonic interactions, as an experimental phenomenon, has been firmly established at RHIC [3]. The challenge for theory is to find an energy loss model built on first principles derivations that *simultaneously* describes the known observables. Currently no such model exists, and there is a debate over the exact, or even dominant, energy loss mechanism at work in the sQGP (see, e.g., [3–5]).

Four observables of interest in leading particle quenching physics are single hadron suppression  $R_{AA}$ ,  $v_2$  (one half the coefficient of the  $\cos(2\phi_s)$  term in the Fourier expansion of the suppression relative to the reaction plane (RP)  $R_{AA}(\phi_s = \phi - \Psi_{RP})$ ), di-hadron suppression  $I_{AA}$ , and  $v_2^{I_{AA}}$ . These observables are interesting because they probe the same energy loss processes in a heavy ion collision, but with different underlying parton spectra and/or path length “ $l$ ” dependencies. For example  $R_{AA}$  at different  $\phi_s$  has identical input parton spectra but explores different path lengths; on the other hand,  $I_{AA}$  probes a harder input spectrum and a different set of paths compared to  $R_{AA}$ . The importance of using multiple observables to constrain the possible energy loss mechanism in heavy ion collisions is well known [6–10]. However, other than one previous publication which examined the

centrality dependence of  $R_{AA}$  vs  $v_2$  [11], the comparison between theory and data was made one observable at a time and usually as a function of  $p_T$  for one centrality selection.

In this work we argue that correlating these observables directly against each other and studying the centrality dependence of the correlation provides novel insights into the high- $p_T$  energy loss mechanism. We propose four types of correlations that can be studied experimentally at RHIC and the LHC:  $R_{AA}$  vs.  $v_2$ ,  $R_{AA}$  vs.  $I_{AA}$ ,  $I_{AA}$  vs.  $v_2^{I_{AA}}$  and  $v_2$  vs.  $v_2^{I_{AA}}$ . We shall first give a brief overview of the experimental measurements of each observable at RHIC. We then explore the main features of the four correlations revealed from the experimental data. Using a jet absorption model, we demonstrate the importance of these correlations by exploring their sensitivities on the geometry and parton spectra shape. We conclude with a discussion of how these correlations can be used to disentangle the “ $l$ ” dependence of energy loss from the collision geometry and parton spectra.

**Overview of experimental results and theoretical comparisons:** The most precise measurements of high- $p_T$  single hadron suppression and anisotropy were carried out by the PHENIX experiment using  $\pi^0$  mesons [12, 13], reaching  $p_T \sim 20$  GeV/c for  $R_{AA}$  and beyond 10 GeV/c for  $v_2$ .  $R_{AA}$  is defined as

$$R_{AA}^h(p_T, \phi_s, b) \equiv \frac{\frac{dN^{AA \rightarrow h+X}}{d^2p_T(p_T, \phi_s, b)}}{N_{bin}(b) \frac{dN^{pp \rightarrow h+X}}{d^2p_T(p_T)}}, \quad (1)$$

where  $N_{bin}(b)$  is the number of binary (hard scattering  $pp$ -like) collisions at impact parameter  $b$ , and  $v_2 \equiv \int d\phi_s R_{AA}(\phi_s) \cos(2\phi_s) / \int d\phi_s R_{AA}(\phi_s)$ . The  $R_{AA}$  shows an almost  $p_T$ -independent factor of 5 suppression in central collisions for  $p_T > 4$  GeV/c. The  $v_2$  drops from 3 to 7 GeV/c, but remains positive at higher  $p_T$ . Current

\*Correspond to jjia@bnl.gov

†Electronic address: wa.horowitz@uct.ac.za

‡Electronic address: jliao@bnl.gov

jet quenching models based on the pQCD framework, when tuned to  $R_{AA}$  data, significantly under-predict the  $v_2$  [13]. In contrast, non-perturbative approaches, for example those based on AdS/CFT gauge gravity duality [14], seem to work well. The data seem to prefer the  $\Delta E \sim l^3$  path length dependence, a result based on AdS/CFT [7], as opposed to the quadratic dependence  $\Delta E \sim l^2$  predicted radiative energy loss predicted by pQCD [15]. Alternatively, a simultaneous description of  $R_{AA}$  and  $v_2$  may also be achieved via a late-stage non-perturbative effect near the QCD confinement transition [11, 16].

The suppression of the away-side jet is quantified by  $I_{AA}$ , the ratio of the per-trigger yield (away-side jet multiplicity normalized by number of triggers) in Au+Au collisions to that in p+p collisions. Pure geometrical considerations would imply  $I_{AA} < R_{AA}$ , due to a longer path length traversed by the away-side jet. But recent PHENIX [17] and STAR [18] measurements show that  $I_{AA}$  is *constant* for associated hadron  $p_T^a > 3$  GeV/c, within the current experimental uncertainties, and this constant level is above the  $R_{AA}$  for the trigger hadrons, i.e.  $I_{AA} > R_{AA}$  (see Fig. 1). Furthermore, the constant level of  $I_{AA}$  increases for higher trigger  $p_T$ . This result can be qualitatively explained by the bias of the away-side jet energy by the trigger  $p_T$ : as we show with a PYTHIA simulation in Fig. 2, the initial away-side jet spectra becomes harder as higher  $p_T$  triggers are required. As we discuss in more detail below, the harder the input spectrum, the larger the fractional energy loss is required for the same  $I_{AA}$  value. The ACHNS model [19] results, constrained by the  $R_{AA}$  data, are incompatible with the  $I_{AA}$  values shown in Fig. 1; while the ZOWW model [20] seems to describe the  $I_{AA}$  data alone shown in Fig. 1, it too fails at simultaneously describing both  $R_{AA}$  and  $I_{AA}$  [21].

PHENIX [22] recently reported the first measurement of the anisotropy of away-side suppression,  $v_2^{I_{AA}} \equiv \int d\phi_s I_{AA}(\phi_s) \cos(2\phi_s) / \int d\phi_s I_{AA}(\phi_s)$ . The away-side yield shows a strong variation with angle of the trigger relative to the RP. This variation is much larger than that for inclusive  $\pi^0$  in the same trigger  $p_T$  range. The current measurement is statistics limited; however the result is tantalizing as energy loss models usually predict much smaller  $v_2^{I_{AA}}$  [22].

**The jet absorption model:** We use a model from [23, 24] to investigate correlations between the four observables, and to check the sensitivities of these correlations to the collision geometry and  $l$  dependence of the energy loss. The model is based on a naïve jet absorption picture where the fractional energy loss of a high  $p_T$  particle is proportional to a line integral  $I$  through the medium,  $\epsilon = \tilde{\kappa}I$ , where  $\epsilon = 1 - p_T^f/p_T^i$ . For a power law production spectrum with index of  $n$ ,  $dN/d^2p_T \sim p_T^{-n}$ ,  $R_{AA}$  is related to the fractional energy loss  $\epsilon = \Delta E/E$  via [25, 26]:

$$R_{AA} = \langle (1 - \epsilon)^{n-2} \rangle \approx \langle e^{-(n-2)\epsilon} \rangle \approx \langle e^{-\kappa I} \rangle, \quad (2)$$

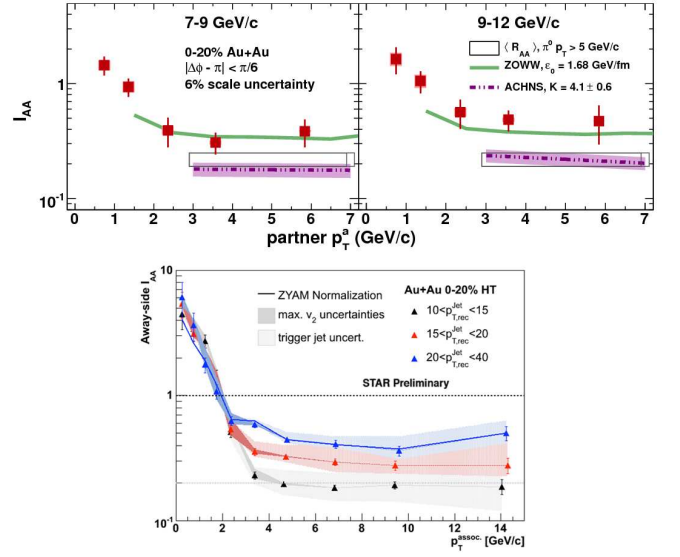


FIG. 1: (Color online) (Top panels) PHENIX  $\pi^0$  -  $h$  correlation results with  $7 < p_T^t < 12$  GeV/c and  $0.5 < p_T^a < 7$  GeV/c [17]. (Bottom panel) the STAR jet-h correlation results with reconstructed trigger jet momentum in  $10 < p_{T,rec}^{jet} < 40$  GeV/c [18]. Both are for the 0-20% Au+Au centrality bin.

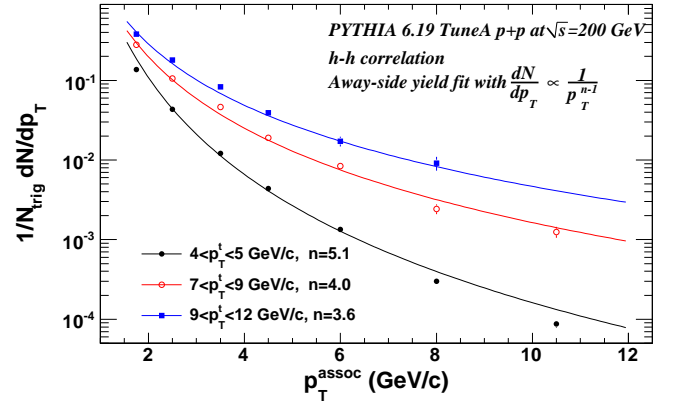


FIG. 2: (Color online) PYTHIA simulation of the away-side per-trigger charged hadron yield spectra in PHENIX  $\eta$  acceptance for three different charged hadron trigger  $p_T$  ranges. The away-side yields are parameterized with a power law function.

where  $\kappa = (n - 2)\tilde{\kappa}$ , and  $\langle \dots \rangle$  indicates an average over the binary collision profile. The line integral  $I$  is calculated as  $I_1 = \int \rho dl$  or  $I_2 = \int \rho l dl$ . The former corresponds to a quadratic dependence of energy loss ( $dE \sim l dl$ ) in a longitudinally expanding medium ( $\rho(\tau) \sim 1/\tau \sim 1/l$ ), while the latter corresponds to a cubic dependence ( $dE \sim l^2 dl$ ) of energy loss in a longitudinally expanding medium. Up to slowly varying logarithmic factors the interference of the unmodified vacuum radiation associated with the production of a high- $p_T$  parton with the medium-induced bremsstrahlung radiation in the deep Landau-Pomeranchuk-Migdal region—

which one expects with the ordering of length scales  $1/\mu \ll \lambda_{mfp} \ll l$  in a weakly-coupled QGP described by Hard Thermal Loop pQCD weakling interacting with the high- $p_T$  parent parton that we might expect in Au+Au collisions at RHIC—yields a fractional energy loss that scales with the square of the pathlength,  $d\epsilon \propto l dl$ . For the not-too-large fractional energy losses at RHIC,  $\langle \epsilon \rangle \sim 0.2$  for  $R_{AA} \sim 0.2$ , the exponential absorption model is a reasonable approximation to the  $1 - \epsilon$  Jacobian expect for pQCD energy loss. On the other hand, under the assumption that all the couplings between the sQGP and the high- $p_T$  parton are very large and the dominant physics can be well approximated using the AdS/CFT conjecture, then the thermalization distance for a light high- $p_T$  probe parton scales as  $E^{1/3}$ . The exponential model can again be used, in this case capturing the physics of the probability of escape for the strongly coupled high- $p_T$  particles. We model the medium density  $\rho$  either by the participant density profile from Glauber geometry or gluon density profile from CGC geometry [27]. The dominant effect of event-by-event fluctuations in the sQGP are included in a medium rotation procedure [28]. Comparison of the jet absorption model to data is a reasonable first step when examining the physics of the centrality dependence of the correlations investigated in this paper as it captures both the pathlength dependence and medium geometry effects.

$\kappa$  is the only free parameter in our energy loss model; we tune it to reproduce  $R_{AA} \sim 0.18$  for 0-5% most central  $\pi^0$ . Once  $\kappa$  is fixed, we then predict the centrality dependence of  $R_{AA}$  in 5% centrality increments, as well as  $I_{AA}$ ,  $v_2$ , and  $v_2^{I_{AA}}$ . The  $\kappa$  values for the four cases (the combinations of  $l^2$ ,  $l^3$  and Glauber, CGC media) are summarized in Table I. Note that for a given “ $l$ ” dependence, the suppression level is essentially controlled by the product of  $\kappa$  and the average matter density  $\langle \rho_{\text{medium}} \rangle \equiv \int \rho(\vec{x})^2 d^2x / \int \rho(\vec{x}) d^2x$  in the 0-5% centrality bin. In general the  $\kappa \langle \rho_{\text{medium}} \rangle$  for CGC geometry is slightly larger than Glauber geometry, primarily because the former has a smaller matter profile [24], while both geometries are assumed to have the same binary collision profile.

TABLE I:  $\kappa$ , average matter density  $\langle \rho_{\text{medium}} \rangle = \int \rho(\vec{x})^2 d^2x / \int \rho(\vec{x}) d^2x$ , and the product of the two in the 0%-5% Au+Au centrality bin, for the four cases calculated in our study.

	$\kappa$	$\langle \rho_{\text{medium}} \rangle$	$\kappa \langle \rho_{\text{medium}} \rangle$
$l^2$ Glauber	0.147	2.96	0.452
$l^2$ CGC	0.076	6.40	0.486
$l^3$ Glauber	0.082	2.96	0.243
$l^3$ CGC	0.046	6.40	0.294

If we assume that the di-hadron production spectrum is also a power law,  $dN/(d^2p_T^a d^2p_T^t) \sim (p_T^a)^{-n_a} (p_T^t)^{-n_t}$

then

$$I_{AA} = \langle (1 - \epsilon_a)^{n_a - 2} (1 - \epsilon_t)^{n_t - 2} \rangle / R_{AA} \approx \langle e^{-\kappa_{\text{away}} I_a} e^{-\kappa I_t} \rangle / R_{AA}. \quad (3)$$

Since  $\kappa \propto n_t - 2 = n - 2$  according to Eq. 2, the effective  $\kappa_{\text{away}}$  for away-side jets should be smaller due to a smaller  $n_a$ . Fig. 2 shows that increasing the momentum of the trigger particle from 4–5 GeV/c to 9–12 GeV/c yields a reduction in the power law for the away-side spectrum from  $n_a = 5.1$  to  $n_a = 3.6$ . One may effectively model this reduction in away-side input spectrum in our absorption model by approximating

$$\kappa_{\text{away}} = \frac{n_a - 2}{n - 2} \kappa; \quad (4)$$

hence the effective strength of the energy loss is reduced by a factor between 2 and 4 for the trigger particle momentum ranges currently measured. One may readily see that as the trigger momentum range is increased, the effects of energy loss on the suppression of particles is reduced;  $I_{AA}$  is not simply smaller than  $R_{AA}$  due to the longer pathlengths that result from the trigger bias in the di-hadron measurement.

**Results:** Fig. 3 (a) shows the predicted correlation between  $R_{AA}$  vs.  $v_2$  from the jet absorption model over the full centrality range. The calculations appear to show little dependence on the assumed geometry (more later), but clearly  $v_2$  increases dramatically from  $l^2$  to  $l^3$  dependence. The  $l^3$  dependence agrees with data well, implying that it can simultaneously describe both  $R_{AA}$  and  $v_2$ , a conclusion already made in [24].

We know that the low- $p_T$   $v_2$  is observed to scale with eccentricity ( $\epsilon$ ) [29]. It was shown in [24] that the jet quenching  $v_2$  also approximately scales with  $\epsilon$ . Thus it is instructive to plot  $R_{AA}$  versus the reduced quantity  $v_{2,r} = v_2/\epsilon$ , as shown in Fig. 3 (b). The data now appear as two sets of points, filled black circles and open red circles, corresponding to Glauber geometry or CGC geometry, respectively. They both indicate an anti-correlation with  $R_{AA}$ , that is a large  $v_{2,r}$  corresponds to a small  $R_{AA}$  and vice versa. Similar trends are also shown by the calculations: as quenching becomes stronger the surviving jets further amplify the initial asymmetry. In Fig. 3 (c) we show the centrality binned theoretical results as open black diamonds and open red crosses for the  $l^3$  Glauber and CGC medium results respectively; these theory points should be directly compared to the filled black circle data points.

Note that while the  $\epsilon \sim l^3$  models with either a CGC medium or Glauber medium appear to describe the  $R_{AA}$  vs.  $v_2$  data in Fig. 3 (a) well, only the cubic model with the CGC medium describes the  $R_{AA}$  vs.  $v_{2,r}$  data shown in Fig. 3 (b). As shown in Fig. 3 (c), this is because the  $l^3$  model with Glauber medium does not describe the data at the *correct centrality bin* whereas the  $l^3$  model with CGC medium does. Eccentricity is a centrality dependent quantity (as discussed in detail in [24]) the CGC

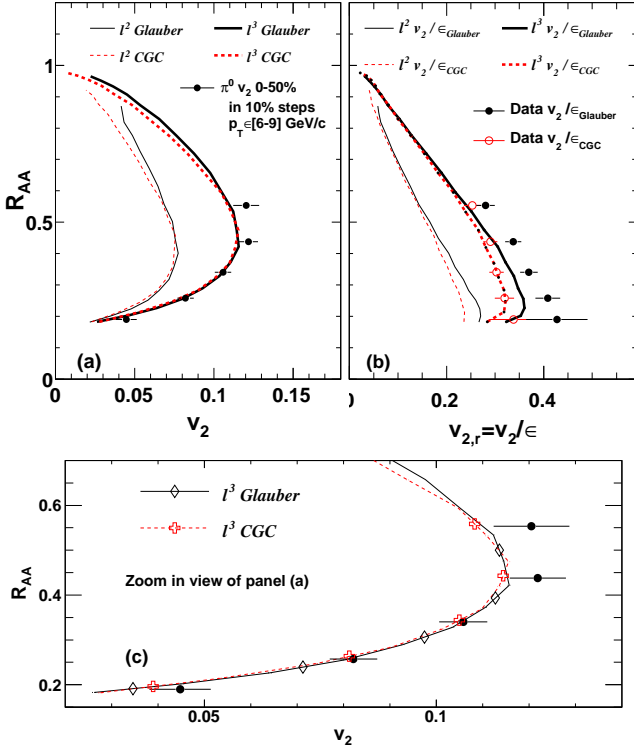


FIG. 3: (Color online) (a) Centrality dependence of  $R_{AA}$  vs.  $v_2$  from the jet absorption model in 5% centrality steps and data (solid circles); only statistical errors are shown. (b) The same data and calculations, except  $v_2$  is divided by the eccentricity. (c) The same as in (a) but zoomed in and with centrality binning explicitly shown for the theoretical results.

geometry is smaller relative to the Glauber geometry), and normalizing with respect to eccentricity has emphasized this mismatch in the centrality-binned results for theory and data. Thus  $R_{AA}$  versus  $v_2/\epsilon$  can better illustrate the relation between jet quenching and azimuthal anisotropy, indicating here that our model only describes the  $R_{AA}$  vs.  $v_2$  data for AdS/CFT-like energy loss in a CGC medium.

Fig. 4 shows the correlation between  $R_{AA}$  and  $I_{AA}$  from the jet absorption model, calculated over the full centrality range. The model results are compared with STAR and PHENIX data from Fig. 1 (0-20% centrality bin) with their  $I_{AA}$  values integrated over  $p_T^a > 3$  GeV/c (where  $I_{AA}$  is flat). In Fig. 4 (a), the data points have roughly the same  $R_{AA}$  value, but are spread out in  $I_{AA}$  for different trigger momenta,  $p_T^t$ . The reason, as explained in the discussion of Fig. 1 & Fig. 2, is that  $I_{AA}$  depends not only on the path length but also on the shape of the input spectra, and the larger the trigger momentum  $p_T^t$  the harder the away-side spectrum. Fig. 4 (a) also shows that  $I_{AA} < R_{AA}$  when only the path length effect is included (i.e. we take  $\kappa_{away} = \kappa$ ). We then attempt to model the effect of the trigger bias on the hardening of the away-side spectrum (see Fig. 2) by using Eq. (4), which yields  $\kappa_{away} = \kappa/2$  in Fig. 4

(b) ( $p_T^t \in [4-5]$  GeV/c),  $\kappa_{away} = \kappa/3$  in Fig. 4 (c) ( $p_T^t \in [7-9]$  GeV/c), and  $\kappa_{away} = \kappa/4$  in Fig. 4 (d) ( $p_T^t \in [9-12]$ ). The toy model improves its agreement with the PHENIX data when both the path length and spectral dependencies are included.

In particular the  $l^3$  AdS/CFT-like energy loss model that described the  $R_{AA}$  vs.  $v_2$  data so well appears to describe the  $R_{AA}$  vs.  $I_{AA}$  data to within about 2-3 standard deviations. One also again sees that the CGC medium yields results whose centrality dependence is in slightly better agreement with the data than the results from the Glauber medium. However it is clear that the  $l^3$  models systematically under-predict the  $I_{AA}$  data. On the other hand the  $l^2$  models tend to disagree more on the level of 1 standard deviation. That the  $l^2$  models tend to describe the normalization and correlation—but not anisotropy—of  $R_{AA}$  and  $I_{AA}$  might suggest the importance of hadronization or flow-coupling effects that are neglected in our model [11, 16, 30].

In general the toy model predicts significantly different  $R_{AA}$  vs.  $I_{AA}$  curves as a function of centrality as a function of trigger momentum: the larger  $p_T^t$  (or, equivalently, smaller  $\kappa_{away}$ ), the more concave the  $R_{AA}$  vs.  $I_{AA}$  curve becomes. The concavity of the correlation is also in general larger for a CGC medium than for a Glauber medium. It would be interesting to see these predictions compared with future measurements performed over the full centrality range in small centrality bins.

The strong suppression of the away-side jet should also lead to an anisotropy of the  $I_{AA}$  relative to the RP. Fig. 5 (a) shows the predicted correlation between  $I_{AA}$  and  $v_2^{I_{AA}}$ , assuming  $\kappa_{away} = \frac{1}{2}\kappa$ . The corresponding correlation between  $I_{AA}$  and reduced anisotropy  $v_{2,r}^{I_{AA}} = v_2^{I_{AA}}/\epsilon$  is shown in Fig. 5 (b). The results for  $\kappa_{away} = \frac{1}{4}\kappa$  are shown in Fig. 5 (c)-(d).

Several interesting features can be identified from the figure. First,  $v_2^{I_{AA}}$  increases dramatically from  $l^2$  to  $l^3$  dependence, but even the  $l^3$  model under-predicts the PHENIX data [22] by about one standard deviation, where the uncertainty is currently very large. Second, calculated  $v_2^{I_{AA}}$  values are very sensitive to  $\kappa_{away}$ : they are larger than the inclusive hadron  $v_2$  of Fig. 3 for  $\kappa_{away} = \frac{1}{2}\kappa$ , but are less for  $\kappa_{away} = \frac{1}{4}\kappa$ . It will therefore be very useful to see experimental results for  $v_2^{I_{AA}}$  as a function of trigger momentum. Finally, we also see a strong anti-correlation between  $v_2^{I_{AA}}/\epsilon$  and  $I_{AA}$ , quite similar to that between  $v_2/\epsilon$  and  $R_{AA}$ . Such similarity may not be surprising if the physics of jet quenching for the trigger and away jets were identical (as in the present model calculation). A precision measurement of these two correlations, therefore, could either confirm such similarity or suggest new physics in the away-side jet quenching.

The correlation between  $I_{AA}$  and  $v_2^{I_{AA}}$  is also quite sensitive to the choice of the collision geometry: switching from Glauber geometry to CGC geometry leads to about a 20% reduction of  $v_2^{I_{AA}}$  and  $v_2^{I_{AA}}/\epsilon$  at fixed  $I_{AA}$



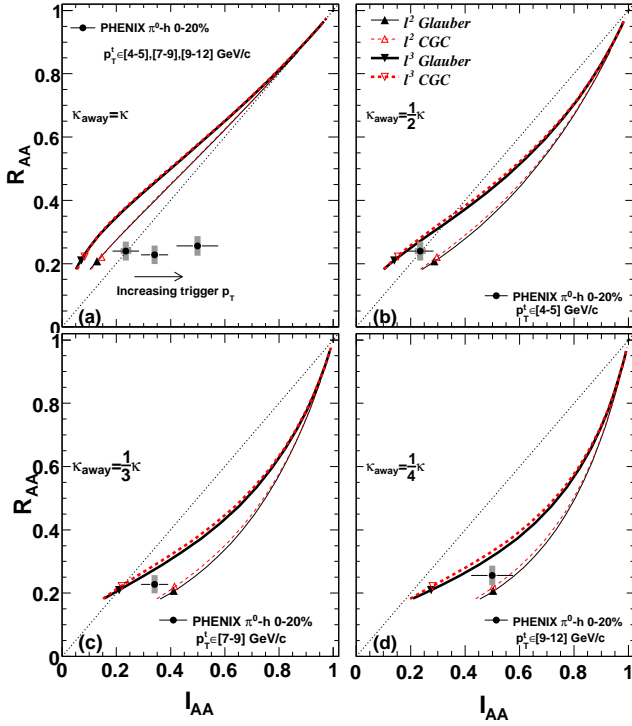


FIG. 4: (Color online) Centrality dependence of  $R_{AA}$  vs.  $I_{AA}$  from the jet absorption model, compared with PHENIX data [17] in the 0-20% centrality bin. The calculations were done assuming  $\kappa$  for away-side jet is (a) the same, (b)  $1/2$ , (c)  $1/3$ , or (d)  $1/4$  of that for inclusive jets. We compare the model curves in (b) to the left-most ([4-5] GeV/c trigger), (c) to the central ([7-9] GeV/c trigger), and (d) to the right-most ([9-12] GeV/c trigger) PHENIX data point. The dotted diagonal line indicates  $I_{AA} = R_{AA}$ . The explicit predictions for 0-20% centrality are shown as diamond and cross symbols.

for  $\kappa_{away} = \frac{1}{2}\kappa$  (significantly smaller for  $\kappa_{away} = \frac{1}{4}\kappa$ ). Thus a precise measurement of this correlation may help in distinguishing between different initial geometries.

Fig. 6 shows the correlation between  $v_2$  and  $v_2^{I_{AA}}$  for  $\kappa_{away} = \frac{1}{2}\kappa$  and  $\kappa_{away} = \frac{1}{4}\kappa$ . Since both observables first increase then decrease from peripheral to central collisions, the correlation plot shows a rather sharp turn at around 20-30% centrality ( $N_{part} \sim 150$ ). This provides a rather precise way of identifying the centrality range at which the anisotropy reaches a maximum. The right panel shows the correlation of reduced anisotropies. We see that all four scenarios fall approximately on a universal curve, especially for  $\kappa_{away} = \frac{1}{2}\kappa$ , but with different reaches along the curve. Apparently, the reach is larger for Glauber geometry and higher order  $l$  dependence. This implies that the efficiency with which jet quenching converts the eccentricity into anisotropy depends on collision geometry and  $l$  dependence. This curve also has an interesting shape: At small  $v_{2,r}$  ( $\lesssim 0.2$  for  $\kappa_{away} = \frac{1}{2}\kappa$  and  $\lesssim 0.3$  for  $\kappa_{away} = \frac{1}{4}\kappa$ ), which corresponds to more peripheral collisions,  $v_2$  is larger than  $v_2^{I_{AA}}$ ; but then  $v_2^{I_{AA}} > v_2$  at large  $v_{2,r}$  ( $> 0.2$  for  $\kappa_{away} = \frac{1}{2}\kappa$  or  $> 0.3$

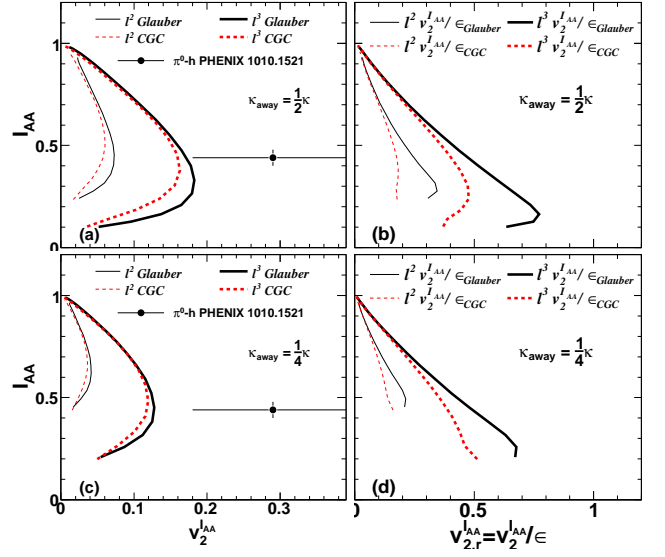


FIG. 5: (Color online) (a) Centrality dependence of  $I_{AA}$  vs.  $v_2^{I_{AA}}$  from jet absorption model in 5% centrality steps and data (solid circles). (b) The same data and calculations, excepts their  $v_2^{I_{AA}}$  have been divided by the eccentricities. (c), (d) are same as (a), (b) but are calculated for  $\kappa_{away} = \frac{1}{4}\kappa$ .

for  $\kappa_{away} = \frac{1}{4}\kappa$ )<sup>1</sup>.

Before closing this section, we want to discuss all correlations together. In general, jet quenching models predict an anti-correlation between suppression and anisotropy ( $R_{AA}$  vs.  $v_2$ , and  $I_{AA}$  vs.  $v_2^{I_{AA}}$ ), while they predict a correlation between the suppressions ( $R_{AA}$  vs.  $I_{AA}$ ) and between the anisotropies ( $v_2$  vs.  $v_2^{I_{AA}}$ ). Thus it is rather surprising to see from the data that  $I_{AA}$  has a larger anisotropy than that for  $R_{AA}$  ( $v_2^{I_{AA}} > v_2$ ), yet it is less suppressed. This feature is very difficult to reproduce in our simple model (see Fig. 4 (d) and Fig. 5 (c)), and, in general, is a challenge for jet quenching theory [21].

**Summary:** The simultaneous description of multiple observables tightly constrains jet quenching models. In this paper we identified four correlations among single hadron and di-hadron observables as useful for constraining jet quenching models:  $R_{AA}$  vs.  $v_2$ ,  $R_{AA}$  vs.  $I_{AA}$ ,  $I_{AA}$  vs.  $v_2^{I_{AA}}$  and  $v_2$  vs.  $v_2^{I_{AA}}$ . Using a jet absorption model, we showed that these correlations are sensitive to various ingredients in the jet quenching calculations, such as the path length dependence, collision geometry, and input spectra shape. Specifically,  $R_{AA}$  vs.  $v_2$  is most sensitive to  $l$  dependence,  $R_{AA}$  vs.  $I_{AA}$  is sensitive to both spectra shape and path length dependence, and  $I_{AA}$  vs.  $v_2^{I_{AA}}$  is sensitive to all three ingredients.

We found that only our energy loss model with  $\Delta E \sim l^3$  AdS/CFT-like energy loss and a CGC medium de-

<sup>1</sup> However for  $l^2$  and CGC geometry,  $v_2 > v_2^{I_{AA}}$  in all centrality bins

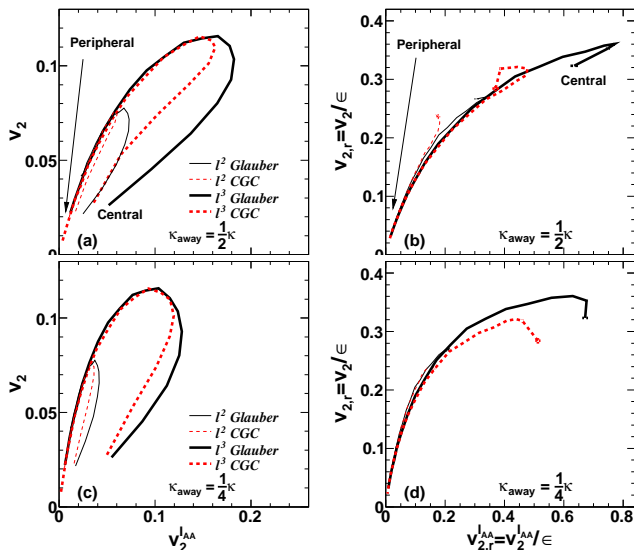


FIG. 6: (Color online) (a)  $v_2$  vs.  $v_2^{IAA}$  and (b)  $v_{2,r}$  vs.  $v_{2,r}^{IAA}$  for 5% centrality steps and four cases for  $\kappa_{away} = \frac{1}{2}\kappa$ . (c), (d) are same as (a), (b) but are calculated for  $\kappa_{away} = \frac{1}{4}\kappa$ . The scaling seen in (b) and (d) is broken in more central collisions as the fluctuations in eccentricity  $\epsilon$  dominate the mean,  $\langle\epsilon\rangle \ll \sqrt{(\epsilon - \langle\epsilon\rangle)^2}$ .

scribes the  $R_{AA}$  vs.  $v_2$  data well as a function of centrality and is also qualitatively (within two to three standard deviations) consistent with the  $R_{AA}$  vs.  $I_{AA}$  data as a function of the trigger  $p_T$ . While the  $l^2$ , pQCD-like energy loss model is completely inconsistent with the  $R_{AA}$  vs.  $v_2$  correlation, the  $l^2$  model describes the  $R_{AA}$  vs.  $I_{AA}$  correlations better than the  $l^3$  model, possibly indicating

important physics such as hadronization or flow-coupling effects missing from our calculation. (Note that the former is unlikely given the very large  $v_2$  values seen at very large  $p_T \sim 10$  GeV/c.) More dynamical calculations of these correlations should provide more quantitative and detailed information, and it is to this end that the proposed correlations should be useful.

We also identified a number of interesting experimental measurements that—once analyzed—will help further constrain energy loss calculations. Our absorption model showed a nontrivial change in the centrality dependence of the  $R_{AA}$  vs.  $I_{AA}$  correlation as a function of the momentum of the trigger particle, due to the hardening of the away-side spectrum; currently there is only a single data point for this correlation for any particular trigger  $p_T$ . Interestingly, the absorption model predicts a universal eccentricity-scaled correlation between  $v_2$  and  $v_2^{IAA}$  for both  $l^2$  and  $l^3$  path length dependencies irrespective of the medium geometry; it would be very interesting to see if this universal relationship is observed in data. Most fascinating is the new correlation measurement between  $I_{AA}$  and  $v_2^{IAA}$ . For the given di-hadron suppression, the very large magnitude of the anisotropy of this suppression cannot be described by either  $l^2$ - or  $l^3$ -type energy loss models. Future measurements that reduce the experimental uncertainty on  $v_2^{IAA}$  may be extremely difficult to reconcile with current notions of high- $p_T$  energy loss physics.

### Acknowledgements

This research is supported by the NSF under award number PHY-1019387.

- 
- [1] M. Gyulassy and L. McLerran, Nucl. Phys. **A750**, 30 (2005), [arXiv:nucl-th/0405013](#).
  - [2] U. A. Wiedemann (2009), [arXiv:0908.2306](#).
  - [3] A. Majumder and M. Van Leeuwen (2010), [arXiv:1002.2206](#).
  - [4] W. A. Horowitz (2010), [arXiv:1011.5965](#).
  - [5] J. Jia (PHENIX), Nucl. Phys. **A855**, 92 (2011), [arXiv:1012.0858](#).
  - [6] H. Zhang, J. Owens, E. Wang, and X.-N. Wang, Phys.Rev.Lett. **98**, 212301 (2007), [arXiv:nucl-th/0701045](#).
  - [7] F. Dominguez, C. Marquet, A. H. Mueller, B. Wu, and B.-W. Xiao, Nucl. Phys. **A811**, 197 (2008), [arXiv:0803.3234](#).
  - [8] S. A. Bass, C. Gale, A. Majumder, C. Nonaka, G.-Y. Qin, et al., Phys.Rev. **C79**, 024901 (2009), [arXiv:0808.0908](#).
  - [9] T. Renk, Phys.Rev. **C78**, 034904 (2008), [arXiv:0803.0218](#).
  - [10] T. Renk and K. Eskola (2011), [arXiv:1106.1740](#).
  - [11] W. A. Horowitz, Acta Phys. Hung. **A27**, 221 (2006), [arXiv:nucl-th/0511052](#).
  - [12] A. Adare et al. (PHENIX), Phys. Rev. Lett. **101**, 232301 (2008), [arXiv:0801.4020](#).
  - [13] A. Adare et al. (PHENIX), Phys. Rev. Lett. **105**, 142301 (2010), [arXiv:1006.3740](#).
  - [14] C. Marquet and T. Renk, Phys. Lett. **B685**, 270 (2010), [arXiv:0908.0880](#).
  - [15] M. Gyulassy and X.-n. Wang, Nucl. Phys. **B420**, 583 (1994), [arXiv:nucl-th/9306003](#).
  - [16] J. Liao and E. Shuryak, Phys. Rev. Lett. **102**, 202302 (2009), [arXiv:0810.4116](#).
  - [17] A. Adare et al. (The PHENIX), Phys. Rev. Lett. **104**, 252301 (2010), [arXiv:1002.1077](#).
  - [18] J. Putschke, talk given at Hard Probes 2010.
  - [19] N. Armesto, M. Cacciari, T. Hirano, J. L. Nagle, and C. A. Salgado, J.Phys.G **G37**, 025104 (2010), [arXiv:0907.0667](#).
  - [20] H. Zhang, J. F. Owens, E. Wang, and X.-N. Wang, Phys. Rev. Lett. **103**, 032302 (2009), [arXiv:0902.4000](#).
  - [21] J. L. Nagle, Nucl. Phys. **A830**, 147c (2009), [arXiv:0907.2707](#).
  - [22] A. Adare et al. (PHENIX) (2010), [arXiv:1010.1521](#).

- [23] A. Drees, H. Feng, and J. Jia, Phys. Rev. **C71**, 034909 (2005), [arXiv:nucl-th/0310044](#).
- [24] J. Jia and R. Wei, Phys. Rev. **C82**, 024902 (2010), [arXiv:1005.0645](#).
- [25] K. Adcox et al. (PHENIX), Nucl. Phys. **A757**, 184 (2005), [arXiv:nucl-ex/0410003](#).
- [26] W. A. Horowitz (2010), [arXiv:1011.4316](#).
- [27] H.-J. Drescher, A. Dumitru, A. Hayashigaki, and Y. Nara, Phys. Rev. **C74**, 044905 (2006), [arXiv:nucl-th/0605012](#).
- [28] B. Alver et al., Phys. Rev. **C77**, 014906 (2008), [arXiv:0711.3724](#).
- [29] A. Adare et al. (PHENIX), Phys. Rev. Lett. **105**, 062301 (2010), [arXiv:1003.5586](#).
- [30] W. A. Horowitz and J. Jia, in preparation.